

## Global Crust-Mantle Density Contrast Estimated from EGM2008, DTM2008, CRUST2.0, and ICE-5G

ROBERT TENZER,<sup>1</sup> HAMAYUN,<sup>2</sup> PAVEL NOVÁK,<sup>3</sup> VLADISLAV GLADKIKH,<sup>1</sup> and PETER VAJDA<sup>4</sup>

**Abstract**—We compute globally the consolidated crust-stripped gravity disturbances/anomalies. These refined gravity field quantities are obtained from the EGM2008 gravity data after applying the topographic and crust density contrasts stripping corrections computed using the global topography/bathymetry model DTM2006.0, the global continental ice-thickness data ICE-5G, and the global crustal model CRUST2.0. All crust components density contrasts are defined relative to the reference crustal density of  $2,670 \text{ kg/m}^3$ . We demonstrate that the consolidated crust-stripped gravity data have the strongest correlation with the crustal thickness. Therefore, they are the most suitable gravity data type for the recovery of the Moho density interface by means of the gravimetric modelling or inversion. The consolidated crust-stripped gravity data and the CRUST2.0 crust-thickness data are used to estimate the global average value of the crust-mantle density contrast. This is done by minimising the correlation between these refined gravity and crust-thickness data by adding the crust-mantle density contrast to the original reference crustal density of  $2,670 \text{ kg/m}^3$ . The estimated values of  $485 \text{ kg/m}^3$  (for the refined gravity disturbances) and  $481 \text{ kg/m}^3$  (for the refined gravity anomalies) very closely agree with the value of the crust-mantle density contrast of  $480 \text{ kg/m}^3$ , which is adopted in the definition of the Preliminary Reference Earth Model (PREM). This agreement is more likely due to the fact that our results of the gravimetric forward modelling are significantly constrained by the CRUST2.0 model density structure and crust-thickness data derived purely based on methods of seismic refraction.

**Key words:** Crust, density contrast, forward modelling, gravity, mantle, moho discontinuity.

### 1. Introduction

The value of  $600 \text{ kg/m}^3$  was traditionally assumed for the crust-mantle density contrast (see e.g., HEISKANEN and MORITZ, 1967, p. 135). MARTINEC (1994) claimed that this value corresponds better with the Moho interface density contrast within the ocean crust, while he estimated the value of  $280 \text{ kg/m}^3$  for the continental crust by minimising the external gravitational potential induced by the Earth's topographic masses and the Moho discontinuity under the assumption that the Moho density contrast is constant. The continental Moho density contrast of  $200 \text{ kg/m}^3$  was reported by GOODACRE (1972) for Canada. The density contrast across the Moho boundary was determined regionally from seismological studies using the wave receiver functions (e.g., NIU and JAMES, 2002 and JORDI, 2007). The results of these studies indicate that the density contrast across Moho may regionally vary as much as from  $160 \text{ kg/m}^3$  (for the mafic lower crust) to  $440 \text{ kg/m}^3$  (for the felsic lower crust), with an apparently typical value for the craton of about  $440 \text{ kg/m}^3$ . DZIEWONSKI and ANDERSON (1981) (Table 1) adopted the value of  $480 \text{ kg/m}^3$  for the global crust-mantle density contrast in the definition of the Preliminary Reference Earth Model (PREM). This value of the crust-mantle density contrast was derived from the seismic reflection data. TENZER *et al.* (2009a) estimated that the average value of the crust-mantle density contrast is about  $520 \text{ kg/m}^3$ . In the most recent study based on solving Moritz's generalisation of the Vening-Meinesz inverse problem of isostasy, SJÖBERG and BAGHERBANDI (2011) estimated that the Moho density contrast varies globally from  $81.5 \text{ kg/m}^3$  in the Pacific region to  $988 \text{ kg/m}^3$  in Tibet, with the average values of  $678 \pm 78$  and  $334 \pm 108 \text{ kg/m}^3$  for the continental

<sup>1</sup> National School of Surveying, University of Otago, 310 Castle Street, Box 56, Dunedin 9054, New Zealand. E-mail: Robert.Tenzer@otago.ac.nz

<sup>2</sup> Delft Institute of Earth Observation and Space Systems (DEOS), Delft University of Technology, Kluyverweg 1, Delft, The Netherlands.

<sup>3</sup> Department of Mathematics, University of West Bohemia, Univerzitní 22, Plzeň, Czech Republic.

<sup>4</sup> Geophysical Institute, Slovak Academy of Sciences, Dúbravská cesta 9, Bratislava, Slovak Republic.

Table 1  
*Statistics of the topographic and crust-stripping corrections to gravity disturbances*

Corrections to gravity disturbances	Min (mGal)	Max (mGal)	Mean (mGal)	RMS (mGal)
Topographic	-661	-17	-69	101
Bathymetric	129	653	332	163
Ice	3	316	22	57
Sediment	14	127	36	23
Upper crust	-124	8	-37	36
Middle crust	-251	-67	-116	46
Lower crust	-532	-115	-188	67

and oceanic areas, respectively. They also estimated that the global average of the Moho density contrast is  $448 \pm 187 \text{ kg/m}^3$ . This estimated value is about 7% smaller than the adopted value ( $480 \text{ kg/m}^3$ ) for the global crust-mantle density contrast in PREM.

The presented study is an update of the article by TENZER *et al.* (2009a) based on using more recent data and more accurate numerical models. The global average value of the crust-mantle density contrast is estimated based on minimising the correlation between the refined gravity and crust-thickness data by adding the crust-mantle density contrast to the adopted reference crustal density. There are two major reasons for estimating the average value of the crust-mantle density contrast. In the context of global studies for a recovery of the Moho density interface from gravimetric data, this value is a required parameter of the functional model formulated between the (known) refined gravity and (unknown) crustal-thickness data. Moreover, when the objective is to study the sub-crustal density distribution anomalies, then the density contrast of the crustal components is usually taken relative to the average density of the lithospheric mantle (upper mantle) estimated based on minimising the correlation between the refined gravity and crust-thickness data. When speaking of the Moho interface density contrast or the crust-mantle density contrast, we have to distinguish between the contrast of the lower-most crust with respect to the encompassing upper-most mantle, and the average crust as a whole with respect to the mantle. The consolidated crust-stripped gravity field (used to estimate the crust-mantle density contrast) describes the refined gravity field generated by the regularised Earth of which all the masses outside the Earth's ellipsoid are removed and the known crust

density distribution is replaced by the homogenous reference crustal density.

We adopt the reference crustal density of  $2,670 \text{ kg/m}^3$ . This value is often assumed for the upper continental crust in geological and gravity surveys, geophysical exploration, gravimetric geoid modelling, compilation of regional gravity maps, and other applications. Although this density value is widely used, its origin remains partially obscure. WOOLLARD (1966) suggested that this density was used for the first time by HAYFORD and BOWIE (1912). In reviewing several studies seeking a representative average density from various rock type formations, HINZE (2003) argued that this value was used earlier by HAYFORD (1909) for gravity reduction. HAYFORD (1909) referred to HARKNESS (1891) who averaged five published values of surface rock density. HARKNESS's (1891) value of  $2,670 \text{ kg/m}^3$  was confirmed later, for instance, by GIBB (1968) who estimated an average density for the surface rocks in a significant portion of the Canadian Precambrian shield from over 2,000 individual measurements. WOOLLARD (1962) examined more than 1,000 rock samples and estimated that the average basement (crystalline) rock density is about  $2,740 \text{ kg/m}^3$ . SUBRAHMANYAM and VERMA (1981) determined that crystalline rocks in low-grade metamorphic terranes in India have an average density of  $2,750 \text{ kg/m}^3$ , while  $2,850 \text{ kg/m}^3$  in high-grade metamorphic terranes. We note here that the choice of the reference crustal density is optional depending on a particular purpose of the numerical study.

The estimation of the crust-mantle density contrast is done using two types of the refined gravity data, namely the consolidated crust-stripped gravity disturbances and the corresponding gravity

anomalies. Whereas the gravity disturbance is defined as a vertical derivative of the disturbing potential, the formulation of the gravity anomaly is based on the fundamental gravimetric equation (cf. VANIČEK *et al.*, 2004, Eq. 9). The second term of the fundamental gravimetric equation represents the distinction between the gravity anomaly and the gravity disturbance. This also has implications in applying the gravity corrections, giving a theoretical foundation for the secondary indirect effects (cf. VAJDA *et al.*, 2006, 2007; and TENZER *et al.*, 2008a, b). As we demonstrate in Sect. 3, the consolidated crust-stripped gravity disturbances differ significantly from the corresponding gravity anomalies due to large contributions of the secondary indirect effects.

The methodology of computing the consolidated crust-stripped gravity data is reviewed in Sect. 2. The results are demonstrated in Sect. 3. The correlation between the refined gravity and crust-thickness data is investigated and the global crust-mantle density contrast is estimated in Sect. 4. The summary of results and conclusions are given in Sect. 5.

## 2. Methodology

The computation of the consolidated crust-stripped gravity disturbances  $\delta g^c$  and the corresponding gravity anomalies  $\Delta g^c$  is done using the following expressions

$$\delta g^c = \delta g - g^t + g^b + g^i + g^s + g^c, \quad (1)$$

and

$$\Delta g^c = \delta g^c - \frac{2}{r}(T - V^t + V^b + V^i + V^s + V^c), \quad (2)$$

where  $r$  is the geocentric radius of the computation point;  $T$  is the disturbing gravity potential;  $\delta g \cong \partial T / \partial r$  is the gravity disturbance and the gravity anomaly  $\Delta g$  is defined by the fundamental gravimetric equation in the following form (e.g.; HEISKANEN and MORITZ, 1967):  $\Delta g = \delta g - 2r^{-1}T$ ;  $V^t$ ,  $V^b$ ,  $V^i$ ,  $V^s$ , and  $V^c$  are, respectively, the gravitational potentials generated by the topography and density contrasts due to the ocean, ice, sediments, and remaining anomalous density structures within the Earth's crust. The respective gravitational attractions

in Eq. 1 are denoted as  $g^t$ ,  $g^b$ ,  $g^i$ ,  $g^s$ , and  $g^c$ . The coefficients of the Earth Gravitational Model 2008 (EGM2008) complete to spherical harmonic degree 180 (PAVLIS *et al.*, 2008) were used to compute the gravity disturbances and gravity anomalies.

The coefficients  $E_{n,m}$  of the global topographic/bathymetric model DTM2006.0 and the coefficients  $N_{n,m}$  of the EGM2008 global geoid model were used to generate the global elevation model (GEM) coefficients  $H_{n,m}$  using the following expression (NOVÁK, 2010)

$$H_{n,m} = E_{n,m} - N_{n,m}. \quad (3)$$

The DTM2006.0 coefficients  $E_{n,m}$  describe the global geometry of the heights above mean sea level (MSL) which are reckoned positive, and the depths below MSL which are reckoned negative. The global topographic/bathymetric model DTM2006.0 was publicly released together with EGM2008 by the US National Geospatial-Intelligence Agency EGM development team. The coefficients  $N_{n,m}$  were generated from the numerical coefficients  $T_{n,m}$  of the disturbing potential (derived from EGM2008) as follows

$$N_{n,m} = \frac{T_{n,m}}{\gamma_0}, \quad (4)$$

where  $\gamma_0$  is the normal gravity at the surface of the reference ellipsoid GRS-80 (MORITZ, 1980). The GEM coefficients complete to degree and order 180 were used to compute the topographic corrections (for a homogenous density of 2,670 kg/m<sup>3</sup>) to gravity data according to expressions derived by NOVÁK (2010).

The coefficients  $E_{n,m}$  and  $N_{n,m}$  were further used to generate the global bathymetric model (GBM) coefficients  $D_{n,m}$  according to the following expression (NOVÁK, 2010)

$$D_{n,m} = N_{n,m} - E_{n,m}. \quad (5)$$

The GBM coefficients complete to degree and order 180 were used to compute the bathymetric stripping gravity corrections. TENZER *et al.* (2011) utilised a depth-dependent seawater density model in deriving expressions for computing these corrections in order to reduce large errors otherwise presented in results when using only a constant seawater density.

The depth-dependent seawater density model was derived by GLADKIKH and TENZER (2011) based on the analysis of the global data of pressure/depth, salinity, and temperature from the World Ocean Atlas 2009 (provided by NOAA's National Oceanographic Data Center; products description can be found in ANTONOV *et al.*, 2010, JOHNSON *et al.* 2009, and LOCARNINI *et al.*, 2010) and the World Ocean Circulation Experiment 2004 (provided by the German Federal Maritime and Hydrographic Agency; see GOURETSKI and KOLTERMANN, 2004). Since the topographic and bathymetric stripping corrections computed using the GEM and GBM coefficients ( $H_{n,m}$  and  $D_{n,m}$ ) according to Eqs. 3–5 are referred relative to the EGM2008 geoid surface, we applied additional corrections due to the gravitational contributions of the topographic and ocean density contrast masses enclosed between the surfaces of the EGM2008 geoid model and the GRS-80 Earth's ellipsoid in order to obtain the ellipsoid-referenced topographic and bathymetric stripping corrections. For more details we refer readers to TENZER *et al.* (2009a); see also VAJDA *et al.* (2008).

The  $10 \times 10$  arc-min mean heights computed by spatial averaging of the  $30 \times 30$  arc-sec global elevation data from GTOPO30 (provided by the US Geological Survey's EROS Data Center) and the  $10 \times 10$  arc-min continental ice-thickness data from ICE-5G (VM2 L90) made available by PELTIER (2004) were used to generate the global ice-thickness model (GIM) coefficients. The GEM and GIM coefficients complete to spherical harmonic degree 180 were used to compute the ice density contrast stripping corrections to gravity data according to expressions derived in TENZER *et al.* (2010b). The density of glacial ice  $917 \text{ kg/m}^3$  (cf. CUTNELL and KENNETH, 1995) was adopted for a definition of the ice density contrast. The accuracy of computed ice density contrast stripping gravity corrections is discussed in TENZER *et al.* (2010b).

For global studies the best currently available global crustal model is CRUST2.0 (BASSIN *et al.*, 2000), which is an upgrade of CRUST5.1 (MOONEY *et al.*, 1998). The CRUST2.0 model contains information on the crustal thickness and the subsurface spatial distribution and density of the following global components: ice; soft and hard sediments; upper, middle, and lower (consolidated) crust. We note here

that the global crust-thickness models CUB2 (SHAPIRO and RITZWOLLER, 2002) and MDN (MEIER *et al.*, 2007) do not provide additional information on the crust density structure. The stripping corrections due to sediments and remaining anomalous crustal density structures were computed using the forward modelling techniques which facilitate the spatial representation of Newton's volume integral. In particular, we applied two integration approaches. The semi-analytical approach was used for computing the far-zone contributions, utilising the Newton–Cotes numerical integration scheme for the surface component of Newton's volume integral, while the vertical component was defined by the closed analytical expression according to GRADSHTEYN and RYZHIK (1980), see also MARTINEC (1998). To reduce the inaccuracy due to using the semi-analytical integration approach, the rectangular prism approach (see NAGY *et al.*, 2000) was utilised for the analytical integration within the near zone up to the distance of 100 km around the observation point. The  $2 \times 2$  arc-deg CRUST2.0 data of density, depth, and thickness of the (soft and hard) sediments and (upper, middle, and lower) crustal components were used to compute globally the stripping gravity corrections due to sediments and consolidated crust components.

### 3. Step-Wise Consolidated Crust-Stripped Gravity Data

We computed and subsequently applied the topographic and crust-stripping corrections to gravity disturbances and gravity anomalies. All computations were realised globally on a  $1 \times 1$  arc-deg geographical grid at the Earth's surface. The density contrasts were taken relative to the reference crustal density of  $2,670 \text{ kg/m}^3$ . The statistics of the topographic and crust-stripping corrections to the gravity disturbances and gravity anomalies are summarised in Tables 1 and 2. The complete corrections to gravity anomalies comprise the combined contribution of the direct and secondary indirect effects. The statistics of the applied secondary indirect effects are given in Table 3. The statistics of the step-wise consolidated crust-stripped gravity disturbances and gravity anomalies are summarized in Tables 4 and 5.

Table 2

*Statistics of the topographic and crust-stripping corrections to gravity anomalies*

Corrections to gravity anomalies	Min (mGal)	Max (mGal)	Mean (mGal)	RMS (mGal)
Topographic	-416	139	42	72
Bathymetric	-598	-132	-374	102
Ice	-54	210	-1	37
Sediment	-68	40	-34	16
Upper crust	-38	82	30	24
Middle crust	8	169	110	29
Lower crust	-52	265	183	42

Table 3

*Statistics of the secondary indirect topographic and crust-components stripping effects*

Secondary indirect effects	Min (mGal)	Max (mGal)	Mean (mGal)	RMS (mGal)
Topographic	69	267	111	35
Bathymetric	-900	-516	-705	101
Ice	-111	-10	-23	23
Sediment	-99	-51	-71	12
Upper crust	34	118	67	21
Middle crust	179	298	226	30
Lower crust	301	495	371	44

Table 4

*Statistics of the step-wise consolidated crust-stripped gravity disturbances*

Gravity disturbances	Min (mGal)	Max (mGal)	Mean (mGal)	RMS (mGal)
EGM2008	-303	293	-1	29
Topographic	-656	275	-70	106
Bathymetric	-519	729	262	230
Ice	-516	732	284	201
Sediment	-496	761	320	197
Upper crust	-549	767	284	229
Middle crust	-797	665	168	270
Lower crust	-1,319	508	20	332

Table 5

*Statistics of the step-wise consolidated crust-stripped gravity anomalies*

Gravity anomalies	Min (mGal)	Max (mGal)	Mean (mGal)	RMS (mGal)
EGM2008	-282	287	-0.5	24
Topographic	-383	341	42	74
Bathymetric	-802	-1	-332	148
Ice	-813	-10	-333	126
Sediment	-868	-47	-367	128
Upper crust	-827	3	-337	148
Middle crust	-804	158	-227	173
Lower crust	-853	392	-44	211

TENZER *et al.* (2009b) demonstrated that the atmospheric correction to gravity disturbances globally varies between  $-0.18$  and  $0.03$  mGal, and the

complete atmospheric correction to gravity anomalies varies from  $1.13$  to  $1.76$  mGal. Since these values are very small compared to the topographic and crust-

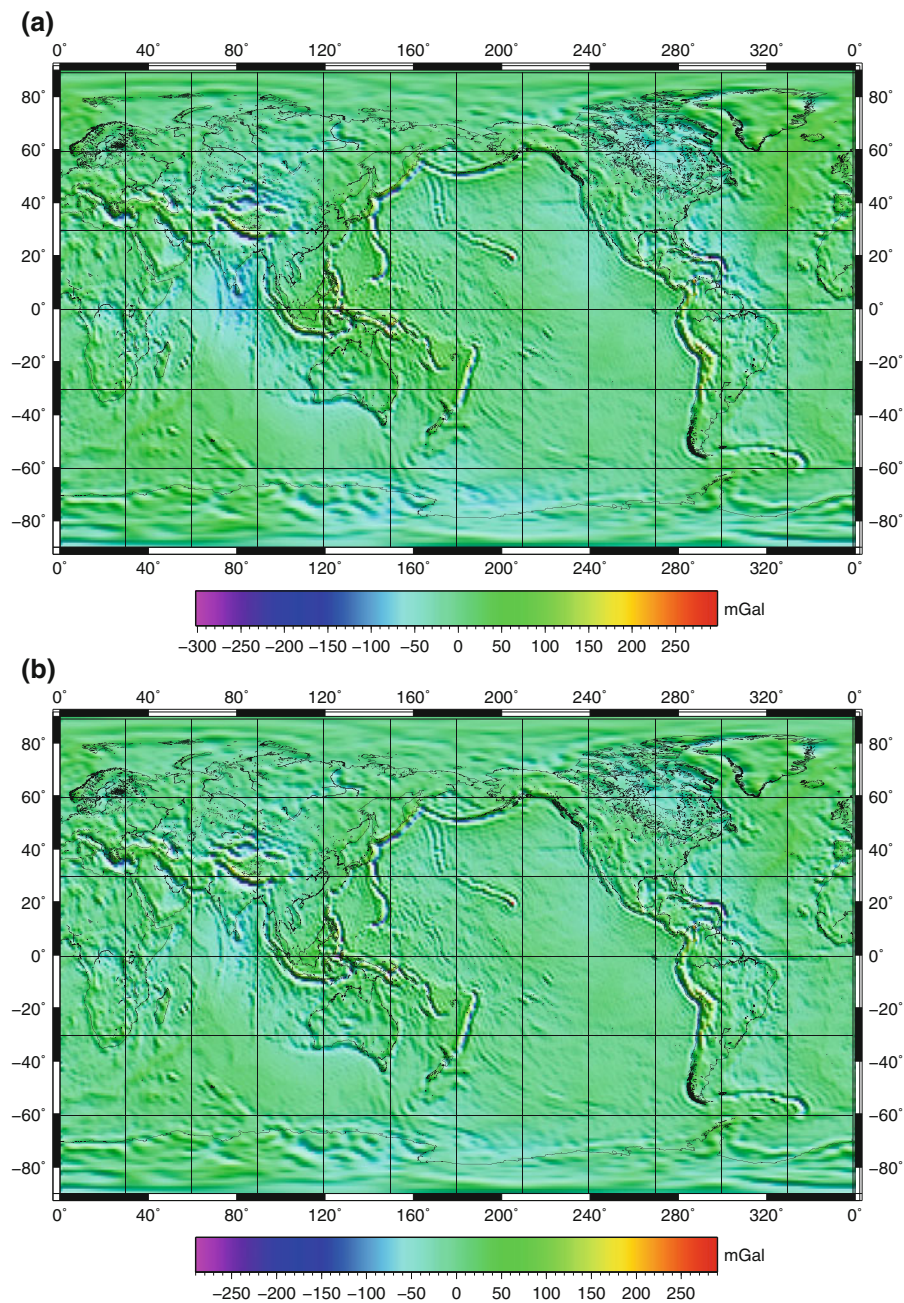


Figure 1

The gravity disturbances (a) and gravity anomalies (b) computed globally on a  $1 \times 1$  arc-deg grid at the Earth's surface using the EGM2008 coefficients complete to spherical harmonic degree 180

stripping gravity corrections (see Tables 1, 2), the gravitational effect of the atmosphere is negligible in the context of this study.

The gravity disturbances and gravity anomalies computed using the EGM2008 coefficients complete to degree 180 of spherical harmonics are shown in

Fig. 1. The topography-corrected gravity disturbances and gravity anomalies are shown in Fig. 2. The application of the topographic corrections to observed gravity data exhibits the isostatic compensation in mountainous regions, where the topography-corrected gravity data have the largest negative

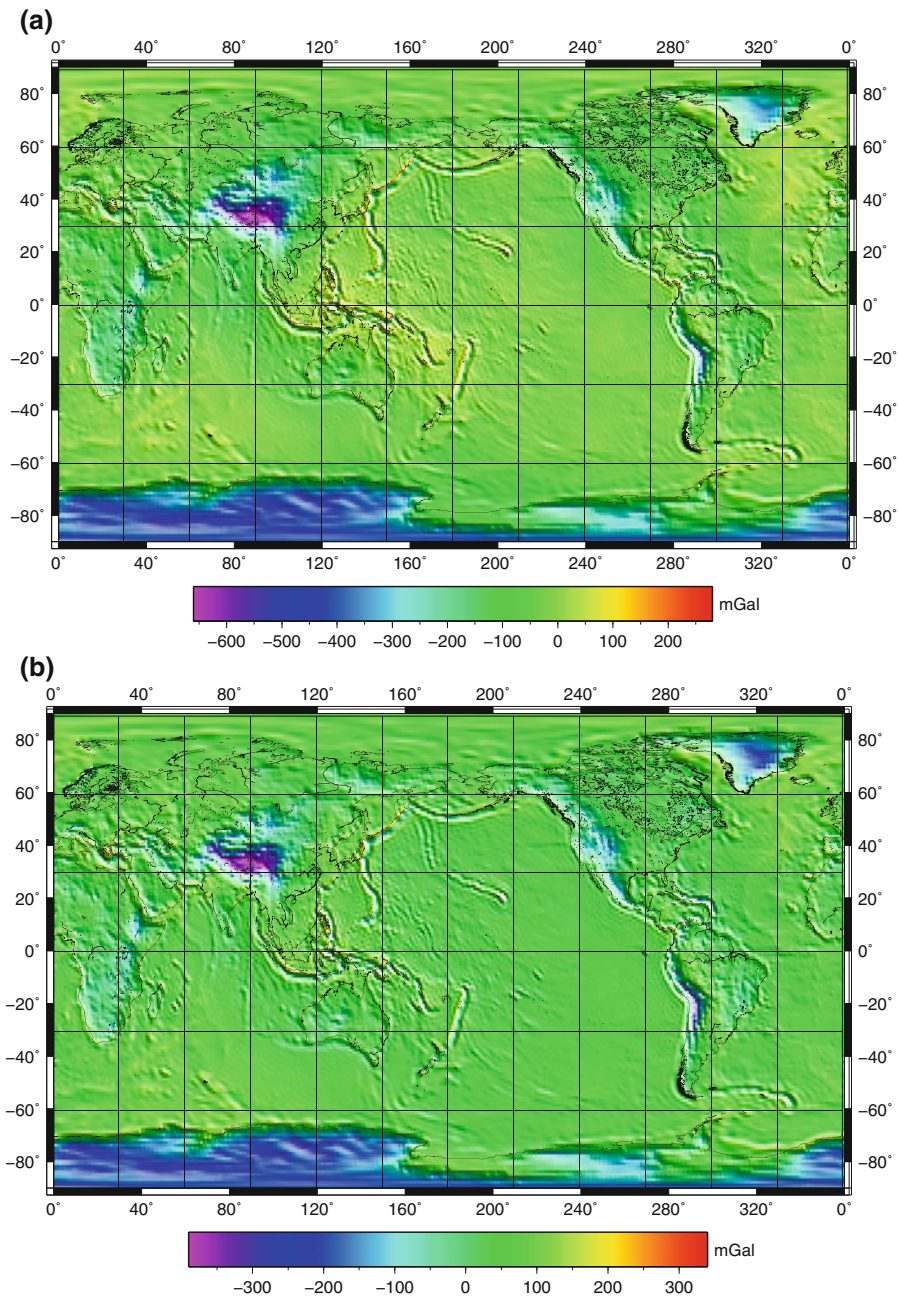


Figure 2

The topography-corrected gravity disturbances (a) and gravity anomalies (b) computed globally on a  $1 \times 1$  arc-deg grid at the Earth's surface using the EGM2008 and DTM2006.0 coefficients complete to spherical harmonic degree 180

values. The largest positive values are mainly located over oceanic areas. The topography-corrected and bathymetry-stripped gravity disturbances and gravity anomalies are shown in Fig. 3. The application of the bathymetric stripping corrections significantly changed the gravity field over oceanic areas and revealed

main structures of the ocean floor relief and the global pattern of the tectonic plates more likely due to the different density and thickness of the continental and oceanic lithospheric plates. Moreover, some features in the gravity signal computed at locations of the world oceans uncovered more detailed features of

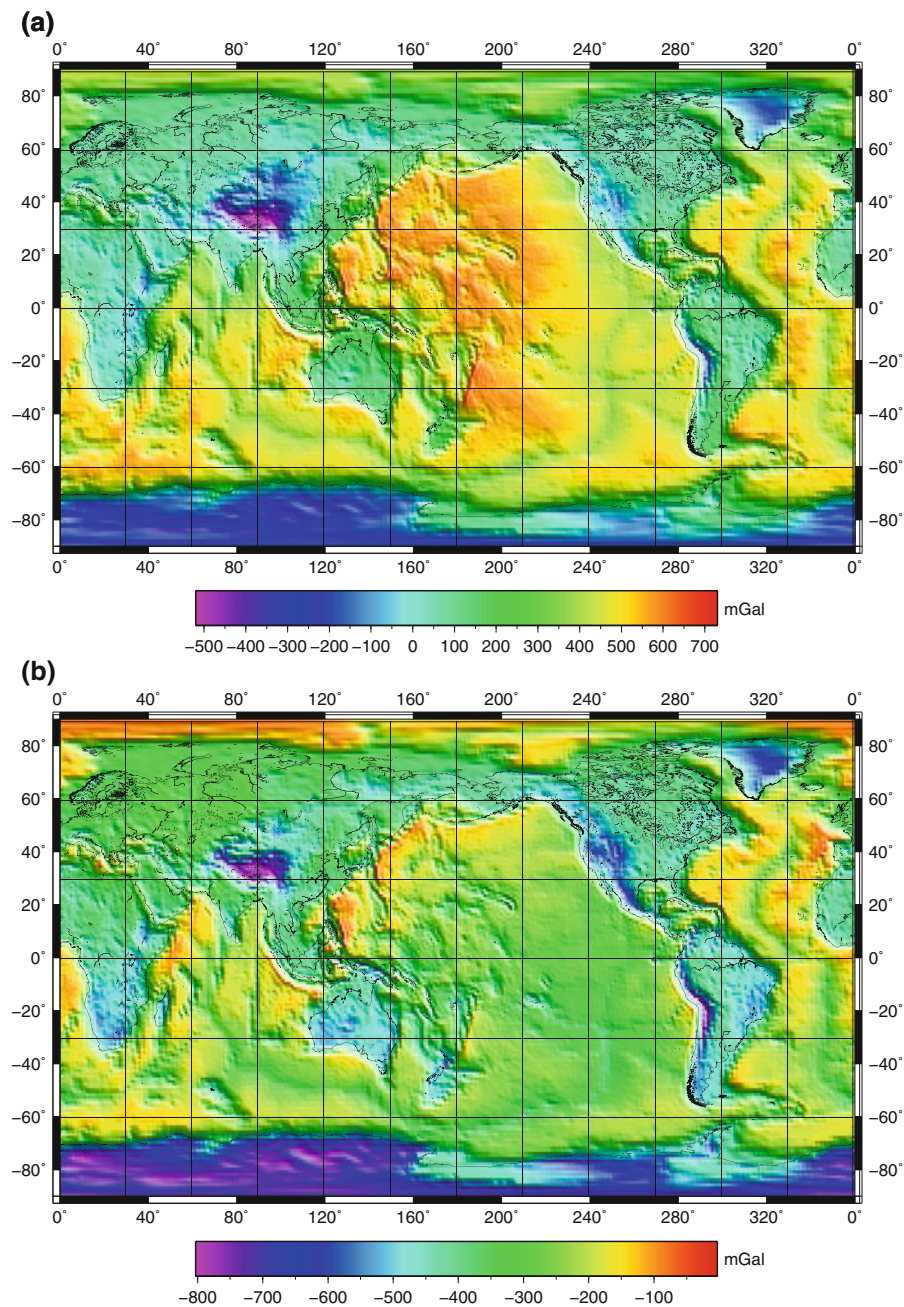


Figure 3

The topography-corrected and bathymetry-stripped gravity disturbances (a) and gravity anomalies (b) computed globally on a  $1 \times 1$  arc-deg grid at the Earth's surface using the EGM2008 and DTM2006.0 coefficients complete to spherical harmonic degree 180

the density and thickness within the oceanic lithospheric plates (for example along the Mid-Atlantic Ridge). Since the bathymetric stripping corrections to gravity data have mostly a long-wavelength character over continental areas, the higher-frequency spectrum

of the topography-corrected gravity data remains almost unchanged. The convergent ocean-to-continent tectonic plate boundaries represent the regions with the largest gravity signal spatial variations. The gravity disturbances and gravity anomalies obtained



after applying the ice density contrast stripping corrections are shown in Fig. 4. The ice density contrast stripping corrections significantly changed the gravity field quantities over the regions with a large thickness

of the continental ice sheet in Greenland and Antarctica. The application of the ice stripping corrections also exhibited more realistically the possible presence of isostasy in the gravity signal over

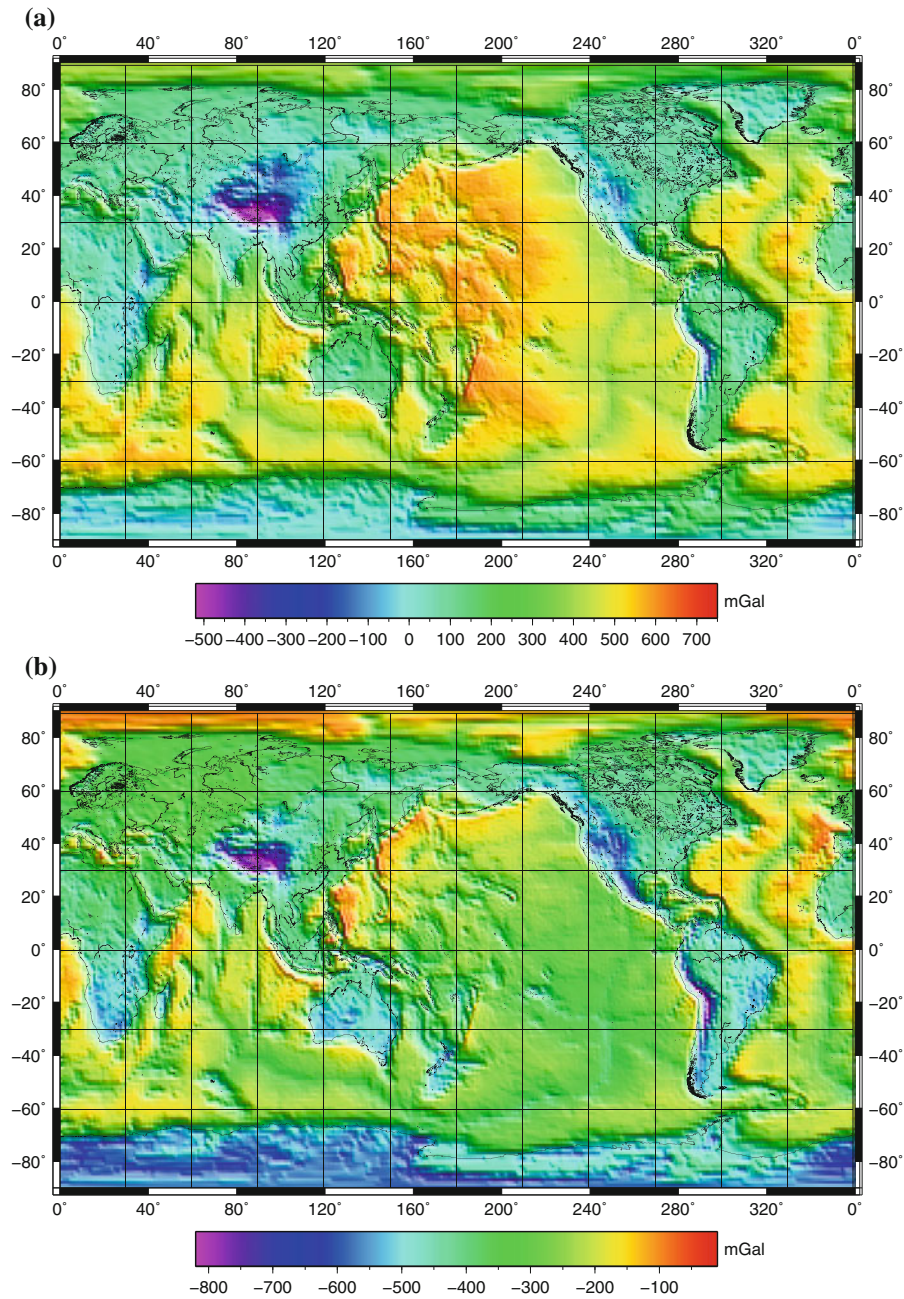


Figure 4

The topography-corrected and bathymetry-, and ice-stripped gravity disturbances (a) and gravity anomalies (b) computed globally on a  $1 \times 1$  arc-deg grid at the Earth's surface using the EGM2008, DTM2006.0, and ICE-5G-derived coefficients complete to spherical harmonic degree 180

the polar continental regions to a large extent magnified after removing the gravitational effect of the topographical masses of density  $2,670 \text{ kg/m}^3$ . The gravity disturbances and gravity anomalies obtained after applying the sediment density contrast stripping

corrections are shown in Fig. 5. The application of the stripping corrections exhibited slightly more the contrast between the continental and oceanic crust in some parts of the world and also slightly changed the pattern of gravity field at the continental shelf regions

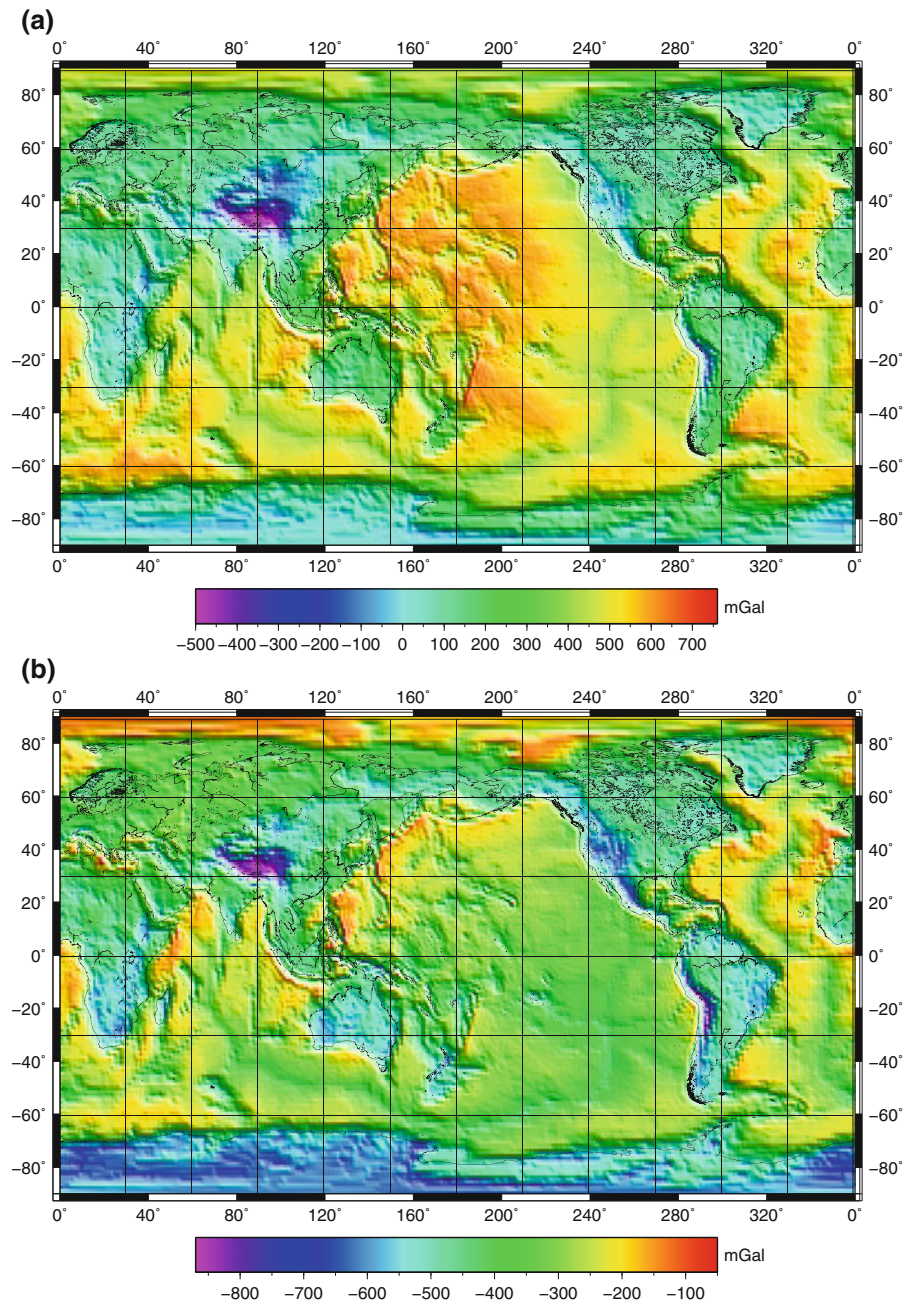


Figure 5

The topography-corrected and bathymetry-, ice-, and sediment-stripped gravity disturbances (a) and gravity anomalies (b) computed globally on a  $1 \times 1$  arc-deg grid at the Earth's surface using the EGM2008, DTM2006.0, and ICE-5G-derived coefficients complete to spherical harmonic degree 180 and the  $2 \times 2$  arc-deg CRUST2.0 data of (soft and hard) sediments density and thickness

with the largest sediment deposits. These changes are, however, not as significant as the corresponding changes in the gravity signal after applying the topographic, bathymetric, and ice stripping corrections due to a relatively small gravitational

contribution of the sediment density contrast (globally mainly below 100 mGal). The consolidated crust-stripped gravity disturbances and gravity anomalies are shown in Fig. 6. The consolidated crust-stripped gravity disturbances globally vary from

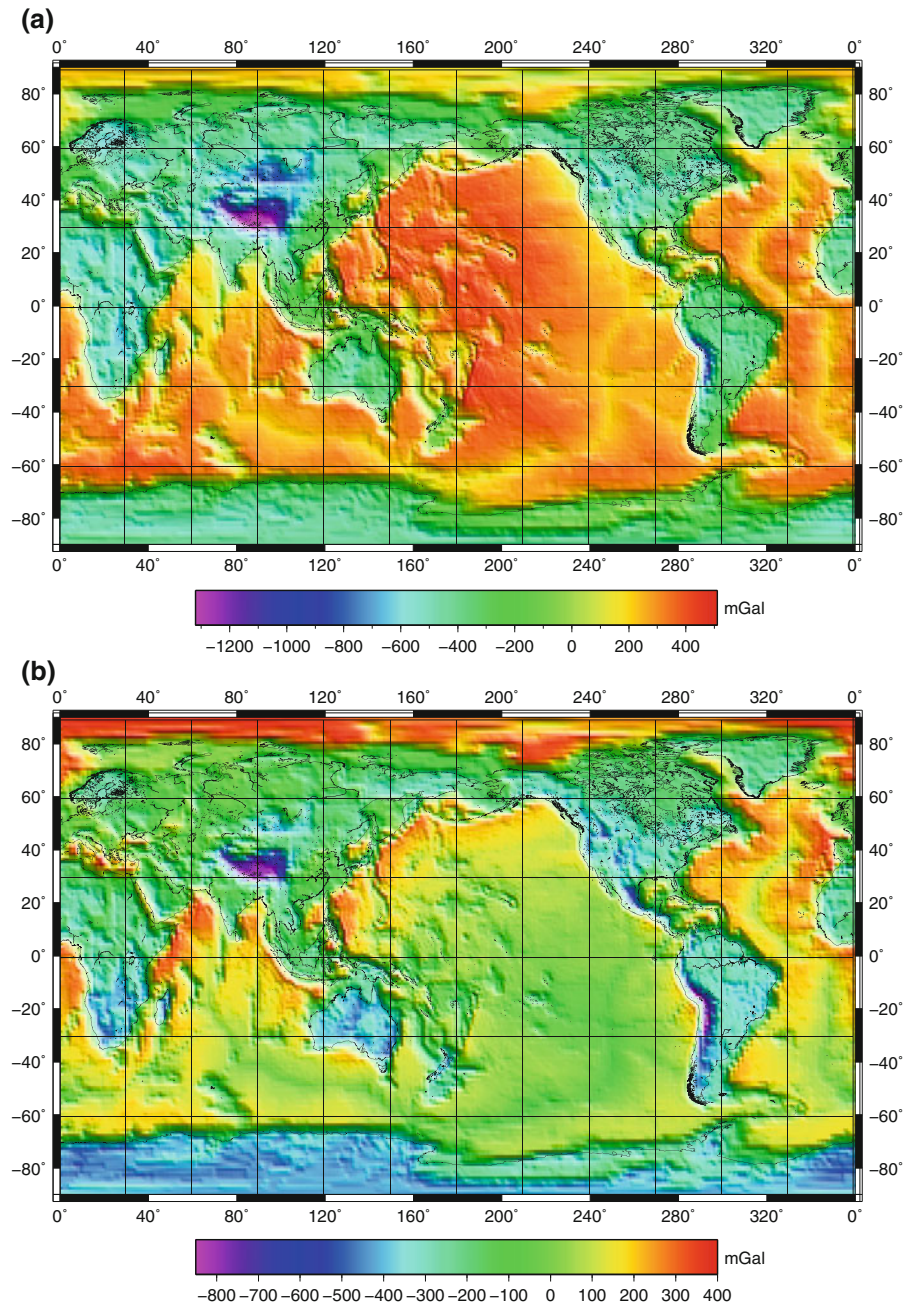


Figure 6

The consolidated crust-stripped gravity disturbances (a) and gravity anomalies (b) computed globally on a  $1 \times 1$  arc-deg grid at the Earth's surface using the EGM2008, DTM2006.0, and ICE-5G-derived coefficients complete to spherical harmonic degree 180, and the  $2 \times 2$  arc-deg CRUST2.0 data of (soft and hard) sediments and (upper, middle, and lower) crust components density and thickness

−1,319 to 508 mGal. The corresponding gravity anomalies vary between −853 and 392 mGal. As seen in Figs. 1 and 6, the differences between the EGM2008 gravity disturbances and gravity anomalies are mostly less than 20 mGal, while these differences reach up to several hundreds of milligals in computed values of the consolidated crust-stripped gravity data. This is due to large contributions of the secondary indirect (topographic and crust density contrasts) effects.

#### 4. Interference of the Crust-Mantle Density Contrast

The correlations between the step-wise refined gravity and crust-thickness data (defined by means of Pearson's linear correlation coefficients) are summarised in Tables 6 and 7. As seen from the results, the consolidated crust-stripped gravity data have the largest correlation with the Moho density interface among all gravity data computed in Sect. 3. We used the  $2 \times 2$  arc-deg global data of the crust thickness taken from CRUST2.0. It is worth mentioning that the differences between the correlations of the gravity field data with the Moho depths (beneath the Earth's

Table 6

*Pearson's linear correlation between the CRUST2.0 crust-thickness data and the step-wise refined gravity disturbances: observed  $\delta g$ , topography-corrected  $\delta g^t$ , topography-corrected and bathymetry-stripped  $\delta g^{bt}$ , and consolidated crust-stripped  $\delta g^c$*

Gravity disturbances	Pearson's correlation
$\delta g$	−0.01
$\delta g^t$	−0.58
$\delta g^{bt}$	−0.89
$\delta g^c$	−0.96

Table 7

*Pearson's linear correlation between the CRUST2.0 crust-thickness data and the step-wise refined gravity anomalies: observed  $\Delta g$ , topography-corrected  $\Delta g^t$ , topography-corrected and bathymetry-stripped  $\Delta g^{bt}$ , and consolidated crust-stripped  $\Delta g^c$*

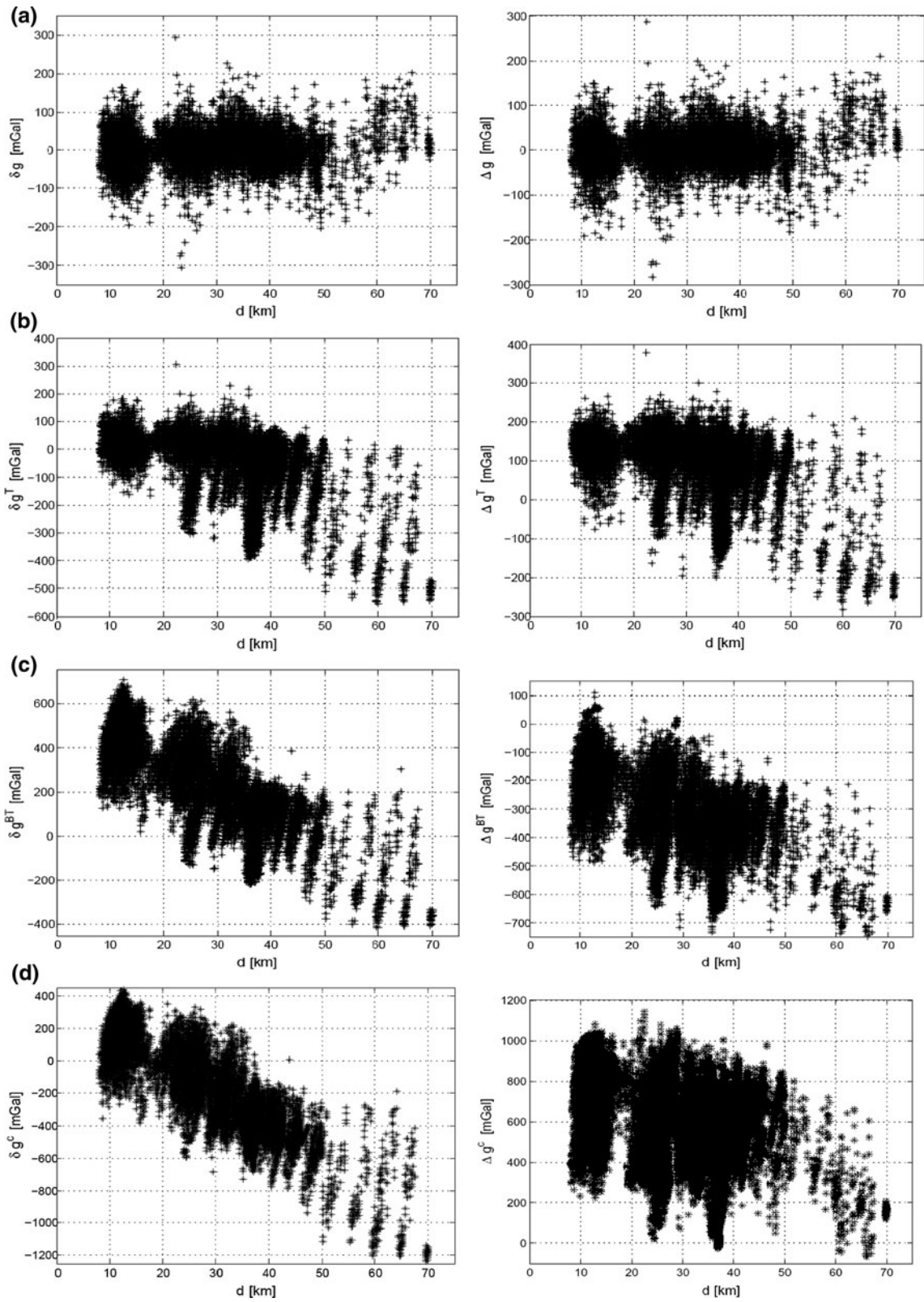
Gravity anomalies	Pearson's correlation
$\Delta g$	0.02
$\Delta g^t$	−0.50
$\Delta g^{bt}$	−0.74
$\Delta g^c$	−0.80

Figure 7

The relation between the CRUST 2.0 crust-thickness  $d$  and the step-wise refined gravity disturbances (*left panels*) and gravity anomalies (*right panels*): **a** observed  $\delta g$  and  $\Delta g$ , **b** topography-corrected  $\delta g^t$  and  $\Delta g^t$ , **c** topography-corrected and bathymetry-stripped  $\delta g^{bt}$  and  $\Delta g^{bt}$ , and **d** consolidated crust-stripped  $\delta g^c$  and  $\Delta g^c$

ellipsoid) and with the entire crust thickness are less than 0.05. Therefore, there would not be any substantial differences in results of the correlation analysis done for the Moho depths instead of using the crust-thickness data. The relation between the crust-thickness and step-wise refined gravity data is shown in Fig. 7. The observed gravity data (computed based on EGM2008) are not correlated with the crust thickness more likely due to the isostatic balance of the Earth's lithosphere. The application of the topographic and bathymetric stripping corrections substantially increased the correlation (in absolute sense) between the gravity and crust-thickness data. The application of the stripping corrections due to ice, sediments, and remaining CRUST2.0 crustal components further increased the absolute correlation between the refined gravity and crust-thickness data up to 0.96 (for the consolidated crust-stripped gravity disturbances) and 0.80 (for the consolidated crust-stripped gravity anomalies).

The consolidated crust-stripped gravity data and the CRUST2.0 crust-thickness data were used to estimate the global average value of the crust-mantle density contrast. This was done by minimising the correlation between the refined gravity and crust-thickness data by adding the crust-mantle density contrast to the original reference crustal density of  $2,670 \text{ kg/m}^3$ . The estimation was carried out individually for the consolidated crust-stripped gravity disturbances and gravity anomalies. As shown in Fig. 8, the correlation between the complete crust-stripped (relative to the mantle) gravity disturbances and the CRUST2.0 crust-thickness reached the absolute minima for the crust-mantle density contrast of  $485 \text{ kg/m}^3$ . The corresponding lowest absolute correlation for the complete crust-stripped (relative to the mantle) gravity anomalies was reached for the crust-mantle density contrast of  $481 \text{ kg/m}^3$ . These values differ significantly from the value of  $520 \text{ kg/m}^3$  estimated by TENZER *et al.* (2009a). This is due to



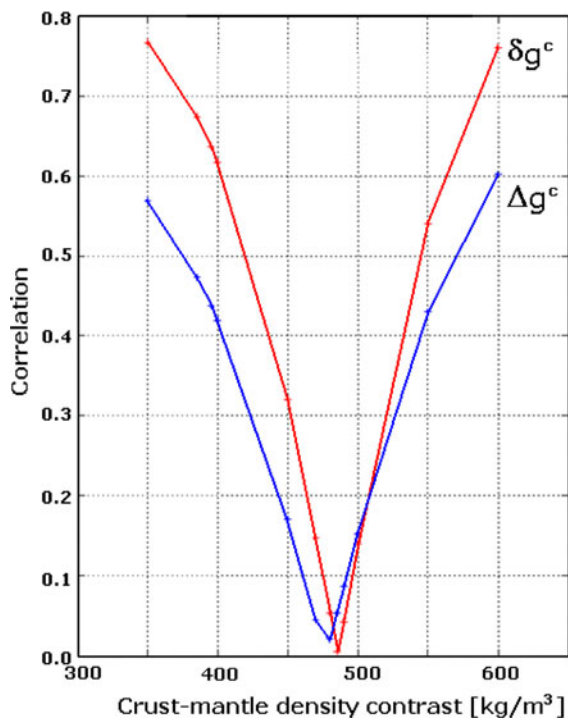


Figure 8

The absolute Pearson's correlation between the complete crust-stripped (relative to the mantle) gravity data and the CRUST2.0 Moho depths data for different values of the crust-mantle density contrast

applying various theoretical and numerical improvements as well as using the latest available global data sets. The most significant theoretical improvement was achieved by adopting the depth-dependent seawater density model in expressions for computing the bathymetric stripping corrections. TENZER *et al.* (2011) demonstrated that the consideration of a depth-dependent seawater density can improve the accuracy in computed values of the bathymetric stripping corrections to about 15 mGal particularly over the open oceans (cf. TENZER *et al.*, 2010a, 2011). The facilitation of the  $10 \times 10$  arc-min continental ice-thickness data from ICE-5G instead of using the  $2 \times 2$  arc-deg CRUST2.0 ice-thickness data improved the accuracy of the computed ice density contrast stripping corrections locally more than 100 mGal. Nevertheless, we anticipate large errors in the computed values of refined gravity field and subsequently in estimated average values of the crust-mantle density contrast. These errors are attributed mainly to the signal of the crustal model uncertainties and the Moho uncertainty

(especially under significant orogens). A realistic assessment of these errors is not simple. KABAN *et al.* (2003) estimated, for instance, that the errors in computed values of the gravitational attraction can reach about 100 mGal over continental regions, while about 40 mGal over the oceanic areas. Moreover, the estimation model would translate also the signal coming from the mantle lithosphere and deeper mantle into false information on the crust-mantle density contrast.

### 5. Summary and Conclusions

We have computed and applied the topographic and crust-stripping corrections to observed gravity data. The step-wise refined gravity data were used for the analysis of the correlation with the crust thickness and for the estimation of the crust-mantle density contrast.

We have demonstrated that the consolidated crust-stripped gravity data have the largest correlation with the crust thickness. Therefore, these refined gravity data are the most suitable (among the investigated gravity data types) for the recovery of the Moho density interface by means of the gravimetric modelling or inversion. Our results revealed that the absolute correlation between the crust-thickness and refined gravity data reached 0.96 and 0.80 for the consolidated crust-stripping gravity disturbances and the corresponding gravity anomalies, respectively.

We have used the consolidated crust-stripped gravity data and the CRUST2.0 crust-thickness data to estimate the global average value of the crust-mantle density contrast. This was done by minimising the correlation between the refined gravity and crust-thickness data by adding the crust-mantle density contrast to the original reference crustal density of  $2,670 \text{ kg/m}^3$ . We obtained the values of  $485 \text{ kg/m}^3$  (for the refined gravity disturbances) and  $481 \text{ kg/m}^3$  (for the refined gravity anomalies). This good agreement between these two estimated values ascertained the correctness of the forward modelling techniques used for a numerical realisation in this study. Our estimated values are very similar to the corresponding theoretical value of  $480 \text{ kg/m}^3$  adopted in the definition of PREM. These values of the

crust-mantle density contrast differ about 7% from the global average of the Moho density contrast of  $448 \text{ kg/m}^3$  estimated by SJÖBERG and BAGHERBANDI (2011) based on solving the Moritz's generalization of the Vening-Meinesz inverse problem of isostasy and by the same amount with respect to a previous assessment (of  $520 \text{ kg/m}^3$ ) by TENZER *et al.* (2009a).

The adopted reference crustal density of  $2,670 \text{ kg/m}^3$  and the estimated value of the crust-mantle density contrast  $485 \text{ kg/m}^3$  (and  $481 \text{ kg/m}^3$ ) yield the value of  $3,155 \text{ kg/m}^3$  (and  $3,151 \text{ kg/m}^3$ ) for the global average density of the upper-most mantle.

### Acknowledgments

Pavel Novák was supported by the Project Plans MSM4977751301 of the Czech Ministry of Education, Youth and Sport. Peter Vajda was supported by the Slovak Research and Development Agency under the contract No. APVV-0194-10 and by Vega grant agency under project No. 2/0107/09.

### REFERENCES

- ANTONOV, J.I., SEIDOV, D., BOYER, T.P., LOCARNINI, R.A., MISHONOV, A.V., GARCIA, H.E. (2010), *World Ocean Atlas 2009*, Vol. 2: Salinity, S Levitus (Ed), NOAA Atlas NESDIS 69, US Government Printing Office, Washington, DC, 184 pp.
- BASSIN, C., LASKE, G., MASTERS, G. (2000), *The current limits of resolution for surface wave tomography in North America*, EOS, Trans AGU, 81:F897.
- CUTNELL, J.D., KENNETH, W.J. (1995) *Physics*, 3rd Edition, Wiley, New York.
- DZIEWONSKI, A.M., ANDERSON, D.L. (1981), *Preliminary Reference Earth Model*. Phys. Earth Planet. Inter. 25, 297–356.
- GIBB, R.A. (1968), *The densities of Precambrian rocks from northern Manitoba*, Canadian Journal of Earth Sciences 5, 433–438.
- GLADKIKH, V., TENZER, R. (2011), *A mathematical model of the global ocean saltwater density distribution*. Pure and Applied Geophysics (submitted).
- GOODACRE, A.K. (1972), *Generalized structure and composition of the deep crust and upper mantle in Canada*, J. Geophys. Res. 77, 3146–3160.
- GOURETSKI, V.V., KOLTERMANN, K.P., *Berichte des Bundesamtes für Seeschifffahrt und Hydrographie* Nr. 35/2004.
- GRADSHTEYN, I.S., RYZHIK, I.M. (1980), *Tables of Integrals, Series and Products*, Translated by Jeffrey A., Academic Press, New York.
- HARKNESS, W. (1891), *Solar Parallax and its Related Constants, including the Figure and Density of the Earth*, Government Printing Office.
- HAYFORD, J.F. (1909), *The Figure of the Earth and Isostasy from Measurements in the United States: U.S. Coast and Geodetic Survey*.
- HAYFORD, J.F., BOWIE, W. (1912), *The effect of topography and isostatic compensation upon the intensity of gravity*, U.S. Coast and Geodetic Survey, Special Publication 10.
- HEISKANEN, W.H., MORITZ, H. (1967), *Physical geodesy*, San Francisco, W.H., Freeman and Co.
- HINZE, W.J. (2003), *Bouguer reduction density, why 2.67?* Geophysics 68(5), 1559–1560; doi:10.1190/1.1620629.
- JOHNSON, D.R., GARCIA, H.E., BOYER, T.P. (2009), *World Ocean Database 2009 Tutorial*, S Levitus (Ed), NODC Internal Report 21, NOAA Printing Office, Silver Spring, MD, 18 pp.
- JORDI, J. (2007), *Constraining velocity and density contrasts across the crust–mantle boundary with receiver function amplitudes*, Geophys. J. Int. 171, 286–301, doi:10.1111/j.1365-2966.2007.3502.x.
- KABAN, M.K., SCHWINTZER, P., ARTEMIEVA, I.M., MOONEY, W.D. (2003), *Density of the continental roots: compositional and thermal contributions*. Earth Planet. Sci. Lett. 209, 53–69.
- LOCARNINI, R.A., MISHONOV, A.V., ANTONOV, J.I., BOYER, T.P., GARCIA, H.E. (2010), *World Ocean Atlas 2009*, Vol. 1: Temperature, S Levitus (Ed), NOAA Atlas NESDIS 68, US Government Printing Office, Washington, DC, 184 pp.
- MARTINEC, Z. (1994), *The Density Contrast At the Mohorovičić Discontinuity*, Geophys. J. Int. 117, 539–544, doi:10.1111/j.1365-246X.1994.tb03950.x.
- MARTINEC, Z. (1998), *Boundary value problems for gravimetric determination of a precise geoid*, Lecture Notes in Earth Sciences, Vol. 73, Springer Verlag, Berlin, Heidelberg, New York.
- MEIER, U., CURTIS, A., TRAMPERT, J. (2007), *Global crustal thickness from neural network inversion of surface wave data*, Geophys. J. Int. 169, 706–722, doi:10.1111/j.1365-246X.2007.03373.x.
- MOONEY, W.D., LASKE, G., MASTERS, T.G. (1998), *CRUST 5.1: A global crustal model at  $5^\circ \times 5^\circ$* , J. Geophys. Res. 103B, 727–747.
- MORITZ, H. (1980), *Advanced Physical Geodesy*, Abacus Press, Tunbridge Wells.
- NAGY, D., PAPP, G., BENEDEK, J. (2000), *The gravitational potential and its derivatives for the prism*, J. Geod. 74, 552–560.
- NIU, F., JAMES, D.E. (2002), *Fine structure of the lowermost crust beneath the Kaapvaal craton and its implications for crustal formation and evolution*, Earth Planet. Sci. Lett. 200, 121–130.
- NOVÁK, P. (2010), *High resolution constituents of the Earth gravitational field*, Surv. Geoph. 31(1), 1–21.
- PAVLIS NK, HOLMES SA, KENYON SC, FACTOR JK (2008), *An Earth Gravitational Model to Degree 2160: EGM 2008, presented at Session G3: "GRACE Science Applications"*, EGU Vienna.
- PELTIER, W.R. (2004), *Global Glacial Isostasy and the Surface of the Ice-Age Earth: The ICE-5G (VM2) Model and GRACE*, Ann. Rev. Earth and Planet. Sci. 32, 111–149.
- SHAPIRO, N.M., RITZWOLLER, M.H. (2002), *Monte-Carlo inversion for a global shear-velocity model of the crust and upper mantle*, Geophys. J. Int. 151, 88–105.
- SJÖBERG, L.E., BAGHERBANDI, M. (2011), *A method of estimating the Moho density contrast with a tentative application by EGM08 and CRUST2.0*, Acta Geophys.
- SUBRAHMANYAM, C., VERMA, R.K. (1981), *Densities and magnetic susceptibilities of Precambrian rocks of different metamorphic grade (Southern Indian Shield)*, J. Geophys. 49, 101–107.

- TENZER, R., HAMAYUN, VAJDA, P. (2008a), *Global secondary indirect effects of topography, bathymetry, ice and sediments*, Contributions to Geophysics and Geodesy 38(2), 209–216.
- TENZER, R., HAMAYUN, VAJDA, P. (2008b), *Global map of the gravity anomaly corrected for complete effects of the topography, and of density contrasts of global ocean, ice, and sediments*. Contributions to Geophysics and Geodesy 38(4), 357–370.
- TENZER, R., HAMAYUN, VAJDA, P. (2009a), *Global maps of the CRUST 2.0 crustal components stripped gravity disturbances*. J. Geophys. Res. 114, B, 05408.
- TENZER R, VAJDA P, HAMAYUN (2009b), *Global atmospheric corrections to the gravity field quantities*. Contributions to Geophysics and Geodesy 39(3): 221–236.
- TENZER, R., VAJDA, P., HAMAYUN (2010a), *A mathematical model of the bathymetry-generated external gravitational field*, Contributions to Geophysics and Geodesy 40(1), 31–44.
- TENZER, R., ABDALLA, A., VAJDA, P., HAMAYUN (2010b), *The spherical harmonic representation of the gravitational field quantities generated by the ice density contrast*, Contributions to Geophysics and Geodesy 40(3), 207–223.
- TENZER, R., NOVÁK, P., GLADKIKH, V. (2011), *On the accuracy of the bathymetry-generated gravitational field quantities for a depth-dependent seawater density distribution*, Studia Geophysica et Geodaetica (accepted).
- VAJDA, P., VANÍČEK, P., MEURERS, B. (2006), *A new physical foundation for anomalous gravity*, Stud. Geophys. Geodaet. 50(2), 189–216, doi:10.1007/s11200-006-0012-1.
- VAJDA, P., VANÍČEK, P., NOVÁK, P., TENZER, R., ELLMANN, A. (2007), *Secondary indirect effects in gravity anomaly data inversion or interpretation*, J. Geophys. Res., Solid Earth, 112, B06411, doi: 10.1029/2006JB004470.
- VAJDA, P., ELLMANN, A., MEURERS, B., VANÍČEK, P., NOVÁK, P., TENZER, R. (2008), *Global ellipsoid-referenced topographic, bathymetric and stripping corrections to gravity disturbance*, Studia Geophysica et Geodaetica 52, 19–34, doi: 10.1007/s11200-008-0003-5.
- VANÍČEK, P., TENZER, R., SJÖBERG, L.E., MARTINEC, Z., FEATHERSTONE, E.W. (2004), *New views of the spherical Bouguer gravity anomaly*, J. Geophys. Int. 159, 460–472.
- WOOLLARD, G.P. (1962), *The relation of gravity anomalies to surface elevation, crustal structure, and geology*, University of Wisconsin Geophysics and Polar Research Center Research Report 62, 9 pp.
- WOOLLARD, G.P. (1966), *Regional isostatic relations in the United States*, In: STEINHART, J.S., SMITH, T.J. (Eds.), *The Earth beneath the continents*, American Geophysical Union Geophysical Monograph 10, 557–594.

(Received February 3, 2011, revised June 5, 2011, accepted August 8, 2011, Published online September 16, 2011)